




RESEARCH ARTICLE

Characterization of differential throughfall drop size distributions beneath European beech and Norway spruce

Marvin Lüpke¹  | Michael Leuchner² | Delphis Levia³  | Kazuki Nanko⁴  | Shin'ichi Iida⁴ | Annette Menzel^{1,5}

¹Professorship of Ecoclimatology, Technische Universität München, Freising, Germany

²Physical Geography and Climatology, RWTH Aachen University, Aachen, Germany

³Department of Geography and Department of Plant and Soil Sciences, University of Delaware, Newark, DE, USA

⁴Department of Disaster Prevention, Meteorology and Hydrology, Forestry and Forest Products Research Institute, Tsukuba, Japan

⁵Institute of Advanced Study, Technische Universität München, Garching, Germany

Correspondence

Marvin Lüpke, Professorship of Ecoclimatology, Technische Universität München, Hans-Carl-von-Carlowitz-Platz 2, 85354 Freising, Germany.
Email: luepke@wzw.tum.de

Abstract

Forest canopies present irregular surfaces that alter both the quantity and spatiotemporal variability of precipitation inputs. The drop size distribution (DSD) of rainfall varies with rainfall event characteristics and is altered substantially by the forest stand properties. Yet, the influence of two major European tree species, European beech (*Fagus sylvatica* L.) and Norway spruce (*Picea abies* (L.) H. KARST), on throughfall DSD is largely unknown. In order to assess the impact of these two species with differing canopy structures on throughfall DSD, two optical disdrometers, one above and one below the canopy of each European beech and Norway spruce, measured DSD of both incident rainfall and throughfall over 2 months at a 10-s resolution. Fractions of different throughfall categories were analysed for single-precipitation events of different intensities. While penetrating the canopies, clear shifts in drop size and temporal distributions of incoming rainfall were observed. Beech and spruce, however, had different DSD, behaved differently in their effect on diameter volume percentiles as well as width of drop spectrum. The maximum drop sizes under beech were higher than under spruce. The mean \pm standard deviation of the median volume drops size (D50) over all rain events was 2.7 ± 0.28 mm for beech and 0.80 ± 0.04 mm for spruce, respectively. In general, there was a high-DSD variability within events indicating varying amounts of the different throughfall fractions. These findings help to better understand the effects of different tree species on rainfall partitioning processes and small-scale variations in subcanopy rainfall inputs, thereby demonstrating the need for further research in high-resolution spatial and temporal properties of rainfall and throughfall.

KEYWORDS

canopy drip, canopy interaction, disdrometer, droplets, interception, rain intensity, rain rate, splash droplets

1 | INTRODUCTION

The size of raindrops has been a curiosity to farmers and scientists alike for over 100 years (e.g., Bentley, 1904). Utilizing a flour pellet method, Bentley (1904) quantified raindrop sizes over his agricultural fields, Vermont, USA. His measurements made intuitive sense because larger raindrops provide more water for crops, and the drop size distribution (DSD) of rain drops is needed to calculate the kinetic energy for soil erosion processes (e.g., Fernández-Raga et al., 2010; Nanko, Hotta, & Suzuki, 2004). In fact, the 1900s were a fertile time for the development of both theoretical advancements and new techniques and instruments to quantify raindrop size and DSD for both rainfall and throughfall (TF) (see Levía, Hudson, Llorens, & Nanko, 2017). Such examples for open rainfall include the Marshall and Palmer (1948) distribution, which is a highly utilized exponential relationship between raindrop size and drop number density related to rainfall intensity, and the first automated DSD instrument (Gunn & Kinzer, 1949). With the use of the flour pellet method, Chapman (1948) is the first known study to examine drop sizes of TF. His primary motivation was to better understand the effects of the forest canopy on soil erosion.

Although different studies have examined the DSD of open rainfall (e.g., L'Ecuyer, Kummerow, & Berg, 2004), the influence of land cover types, such as forests, on DSD is not yet fully understood. Forest canopies intercept incident rainfall and thus change the rainfall distribution and its amount (Crockford & Richardson, 2000); consequently, their TF DSD differs from open precipitation (Hall & Calder, 1993). With the advent of optical disdrometers, a number of studies have begun to examine the effects of meteorological conditions, canopy structure, and the role of plant surfaces on TF DSD (e.g., Frasson & Krajewski, 2011; Hall & Calder, 1993; Nanko, Hotta, & Suzuki, 2006; Nanko, Hudson, & Levía, 2016; Nanko, Watanabe, Hotta, & Suzuki, 2013; Zabret, Rakovec, Mikoš, & Šraj, 2017 summarized in Levía et al., 2017). These studies investigated the following species: *Zea mays* L. (maize; Frasson & Krajewski, 2011), *Pinus caribaea* Morelet (Caribbean pine), *Eucalyptus camaldulensis* D. (river red gum), and *Tectona grandis* L. F. (Teak; Hall & Calder, 1993) as well as *Chamaecyparis obtusa* (Siebold & Zucc.) ENDL (Japanese cypress), *Cryptomeria japonica* (Thunb. ex L. F.) D. Don (Japanese red cedar), and *Quercus acutissima* Carruth. (sawtooth oak; Nanko et al., 2006). Yet, until now, major European tree species, such as *Fagus sylvatica* L. (European beech; Trucchi & Andrenelli, 2007) and *Picea abies* (L.) H. Karst. (Norway spruce; Armstrong & Mitchell, 1987; Ovington, 1954), have not been investigated on a longer time scale under ambient conditions with a laser disdrometer.

Past studies have shown that TF DSD may be categorized into (a) drip (TF_d), which is generated by the accumulation of intercepted raindrops on leaves (Mosley, 1982) and branches (Nanko et al., 2006) and is characterized by larger drops. These drops can have a higher kinetic energy but are smaller in number (Nanko et al., 2004) and (b) splash or impact droplets (TF_s), which result from the impact of drops on the canopy surface (Herwitz, 1987) and (c) free TF (Levia et al., 2019; Moss & Green, 1987). However, kinetic energy

depends highly on the released height of the droplet, therefore, under tree canopies, drops can accelerate to terminal velocity and have the full kinetic impact (Gunn & Kinzer, 1949), whereas under lower canopies such as maize, the full terminal velocity is not reached (Frasson & Krajewski, 2011). In addition, the accumulation process in form of dripping spots (e.g., end of branch or leaf; Nanko et al., 2013) might favour local erosion processes.

These TF_s have smaller diameters than TF_d but are much larger in number (Levia et al., 2019; Nanko et al., 2006). The unaltered drops that pass through the canopy are termed free TF. Despite these insights, there is still much to learn about TF DSD (Levia et al., 2017), especially with regard to interspecific differences between deciduous and coniferous tree species under natural conditions.

The primary goal of this study is to examine the differences in TF DSD beneath the canopies of two major European tree species, European beech and Norway spruce, with inherently different three-dimensional canopy structures under natural rainfall events at a single-measurement location at a high temporal resolution. Given the fact that median TF drop size appears to be larger under leafless than leafed conditions when structurally created canopy drip points become more pronounced without the presence of foliage (Nanko et al., 2016), we seek to delve into the interspecific differences in TF DSD between these two species during the growing season in order to better understand how different canopy structures affect TF DSD. We also examine the effects of meteorological conditions of rainfall on TF DSD beneath both beech and spruce and how TF DSD changes over the course of particular rain events.

Given the fact that TF is a major input of water and solutes to the forest floor (Levia & Frost, 2006) and drip constitutes larger water volumes (Levia et al., 2019), a better understanding as to how much TF is divided into splash and drip components is necessary to quantify the amounts (and spatial heterogeneities) of TF inputs to the forest floor that can affect soil respiration (Liu et al., 2016), nitrous oxide emissions (Davidson, Ishida, & Nepstad, 2004), and soil erosion (Shinohara, Ichinose, Morimoto, Kubota, & Nanko, 2018). Our work represents an initial step in being able to link the type of TF inputs to water-mediated processes in the forest soil. For example, do locations with larger canopy drip input have higher soil moisture levels and higher levels of soil respiration? An answer to this and similar questions would allow hydrologists and biogeochemists a more precise ability to pinpoint hot spots of carbon cycling on the forest floor. Accordingly, a closer examination of differential TF dynamics beneath deciduous and coniferous species during the growing period is a first step to increase our process-based understanding of TF generation that could provide insights to improve knowledge of forest–water interactions that may influence larger biogeochemical cycles in forests.

2 | MATERIALS AND METHODS

2.1 | Experimental set-up and site

The measurements were conducted at the “Kranzberger Forst” experimental site located about 35 km north-east of Munich, Germany

(48°25'08"N, 11°39'41"E, 485 m a.s.l.). The mixed mature stand of European beech and Norway spruce is specified by a projected leaf area index at full foliation of around $6 \text{ m}^2 \text{ m}^{-2}$ for both beech and spruce (Reiter, 2004). Height measurements in 2008/2009 by Kuptz, Matyssek, and Grams (2011) and age determination in 2010 by Pretzsch et al. (2014) showed for spruce a mean height of $28.8 \pm 0.8 \text{ m}$ with an age of 59 ± 2 years and for beech a height of $25.9 \pm 0.3 \text{ m}$ with an age of 79 ± 2 years, respectively.

A maximum leaf area density of $6 \text{ m}^2 \text{ m}^{-3}$ for beech was measured in the upper third and up to $2.6 \text{ m}^2 \text{ m}^{-3}$ for spruce in the lower half of the canopy (Häberle et al., 2003). The basal area was $46.4 \text{ m}^2 \text{ ha}^{-1}$, whereas the stand density was $764 \text{ stems ha}^{-1}$ (Wipfler, Seifert, Heerdt, Werner, & Pretzsch, 2005). The height of the branches of the lower edge of the crown ranged between 14.5 and 20.3 m for both species (Reiter, 2004). Leaf width between both species at this site were reported by (Reiter et al., 2005) at around 0.1 cm for spruce and 3.5/5.3 cm for beech (shade/sun leaf) and a specific leaf area ranging from 3.3 to $5.6 \text{ m}^2 \text{ kg}^{-1}$ (spruce) and 11.0 to $36.6 \text{ m}^2 \text{ kg}^{-1}$ (beech), respectively. Length was only measured for spruce with an average of 12.6 mm per needle (Reiter et al., 2005).

Two PARSIVEL disdrometers (OTT Hydrology, Germany) were used to obtain hydrometeor size and velocity below and above the canopy to derive the DSD changes by the canopy. The PARSIVEL is based on the principle described by Löffler-Mang and Joss (2000) using a laser beam to measure the length and amplitude of a voltage signal created by the extinction of a crossing particle. The diameter is calculated based on a linear relation of particle size to the amplitude. Both devices are precalibrated by the manufacturer with known particle sizes and velocities. Size is derived by measuring the amplitude and converting it into a corresponding diameter. The particle velocity is retrieved from the duration of the signal decay of each particle while passing the laser beam.

After size and velocity calculation, each measured particle is assigned into a corresponding diameter velocity class. These diameter classes range from 0.3 to 24.5 mm (compared with the maximum of 6.0 mm from the Hall and Calder (1993) study and 8.0 mm from the Nanko et al. (2006) study and velocity classes from 0.050 to 20.800 m s^{-1} , which result into a 32×32 matrix. However, the version of the deployed disdrometer could not account for the first two diameter classes (class diameter mean: 0.062 and 0.187 mm) due to a bad signal to noise ratio (Löffler-Mang & Joss, 2000). Both devices above and below canopy were connected with a computer to guarantee time-synchronized recording in a 10-s interval. For ensuring the same mode of operation of both disdrometers, firmware on both devices was updated to the same version (1.17).

The above-canopy disdrometer was placed on top of a 34-m high tower. In order to minimize masking effects of the device at higher wind speeds (Upton & Brown, 2008), the disdrometer was oriented perpendicular to the main wind direction (W-E). The second device was installed at a 2-m mast on the forest floor below the canopy of spruce or beech, respectively. For each tree species, the disdrometer was placed at around the mid-crown radius. Its horizontal distance to the tower was about 15.9 m for the pure beech group and 19.5 m for

the pure spruce group. This close set-up of both disdrometers guaranteed a short temporal lag between tower and ground position as well as a spatial closeness; thus, intraevent properties would not change significantly. However, due to two separated time periods for each species, we suspected different abundance of rain events and types. Due to the limited number of disdrometers, this set-up was not able to cover the high spatial variability present within a stand and under the canopy, respectively. The focus was set on temporal changes of DSD and the effect of different rainfall events.

Measurements under beech were taken from mid-July to mid-August and under spruce from mid-August to mid-September 2010 when all leaves were completely developed. Due to some electronic failures, neither disdrometer provided full continuous measurements during the operation period; however, a sufficient number of complete rain events (see Section 2.3 for definition) was captured.

2.2 | Data processing

The experiment aimed to investigate DSD change resulting from canopy influences; for that purpose, we used the raw drop size and velocity distribution data as recorded by the PARSIVEL, because the automatically computed data only contained some of the desired parameters. However, due to different fringe effects of optical disdrometers (Battaglia, Rustemeier, Tokay, Blahak, & Simmer, 2010) caused by non-hydrometeor particles or simultaneously crossing particles, for example, raw DSD can include errors. In contrast, the computed variables by the PARSIVEL internal software such as rain rate (RR) and rain amount (RA) are corrected for these effects. An implementation of a similar correction algorithm into our raw data processing was not done, because the normal assumption on open rainfall distribution in terms of size and velocity is not appropriate under the canopy. Correction of large particles, for example, which probably would not occur in rainfall DSD, but can occur under the canopy, would lead to a loss of information in this case and an error in the measurement (Raupach & Berne, 2015).

RA (mm) was calculated for each diameter class, interval, and event. The drop number N was aggregated for intervals and events. RR (mm hr^{-1}) was computed for each interval and event. For comparison of the different DSD of each event, the RA was normalized to the total RA measured by the tower disdrometer.

In order to characterize DSD, we used three percentile volume diameters, D10, D50, and D90, calculated according to the equation by Nanko et al. (2016) in Equation (1):

$$D50 = D_{m1} + \frac{\frac{1}{2} \sum_i^c n_i V_i - \sum_i^{m1} n_i V_i}{\sum_i^{m2} n_i V_i - \sum_i^{m1} n_i V_i} (D_{m2} - D_{m1}), \quad (1)$$

where c is number of diameter classes, n_i the number of drops per diameter class, V_i the volume per diameter class, D_{m1} the diameter class below the 50% cumulative volume, and D_{m2} the diameter above the 50% cumulative volume. For D10 and D90, Equation (1) was adapted according to the 10th and 90th percentiles.

The median volume diameter D50 is often used to represent the entire DSD (Sempere-Torres, Porrà, & Creutin, 1998), and it is used to compare DSD under different canopy species (Brandt, 1989; Hall & Calder, 1993; Levia et al., 2019; Nanko et al., 2006). In order to get a robust D50, only high intensity or long events with high-drop numbers would be suitable (Salles, Poesen, & Borselli, 1999), but the natural rain contain a high variability compared with controlled artificial rain. In our study, we further analysed also small scale/light intensity events and even single-measurement intervals with higher variability to gain more insight into DSD change under the canopy and, thus, also kept events with lower drop numbers.

Because of rainfall redistribution by the canopy, the below canopy spectrum shows a different DSD (Nanko et al., 2006) in the lower and higher diameter ranges than the typical for open rainfall. Thus, two additional diameter volume percentiles for the 10th (D10) and 90th (D90) volume amount were introduced. D90 can be used to represent the dripping fraction and D10 to represent the splashing fraction better than D50. All parameters were computed for each 4-min interval during an event and for the entire event (see Section 2.3 for definition of events).

The second goal of this study was a more detailed description of TF and its fractions. The additional information from both disdrometers can be used to achieve this.

Due to the spectral change below the canopy, parts of the DSD can be separated into different TF fractions: TF with splash droplets (TF_s), TF composed of canopy drip (TF_d), mixed fraction TF_{mix} , containing free TF as well as release TF, not distinguishable from TF_d or TF_s . With the TF_{mix} component inherent to this study, it employed a different TF partitioning approach than Levia et al. (2019).

Figure 1 shows the separation of the total RA measured at floor below the canopy into the different stand precipitation fractions. This was done by subtracting the understory volume ($RA_{floor\ i}$) per diameter class i from the above canopy layer ($RA_{open\ i}$):

$$DIFF_i = RA_{open\ i} - RA_{floor\ i} \quad (2)$$

If $DIFF_i < 0$, we can assume that either splash droplets (<1 mm; TF_s) or drip (≥ 2 mm; TF_d) were produced. Several studies showed that splash droplets were detected at around 1 to 2 mm and drip above the 1 mm diameter (e.g., Nanko et al., 2006; Yang & Madden, 1993), and also, the study of Nanko et al. (2016) showed that minimum diameter of drip can range between 1 and 2 mm. Therefore, diameters between 1 and 2 mm cannot be attributed to either splash or drip and can be a mixture. Because this mechanism is a smooth transition and depending on various factors, a fixed factor is difficult to determine but necessary for classification.

Both TF components were calculated by

$$TF_{s\ i} = |DIFF_i| : \text{drop diameter} < 1\text{mm} \bigwedge DIFF_i < 0, \quad (3)$$

$$TF_{d\ i} = |DIFF_i| : \text{drop diameter} \geq 2\text{mm} \bigwedge DIFF_i < 0. \quad (4)$$

TF_{mix} was calculated by

$$TF_{mix\ i} = RA_{floor\ i} - |DIFF_i| : DIFF_i < 0, \quad (5)$$

$$TF_{mix\ i} = |DIFF_i| : \text{drop diameter} \geq 1 \bigwedge < 2\text{mm} \bigwedge DIFF_i < 0, \quad (6)$$

$$TF_{mix\ i} = RA_{floor\ i} : DIFF_i > 0. \quad (7)$$

On a whole event scale, the difference between rainfall and TF was used as proxy for interception loss and stemflow.

All fractions for each diameter class were aggregated into values for a 4-min interval or the whole event. With 4-min intervals, we have to assume transfer between each interval, which is not separable with this method.

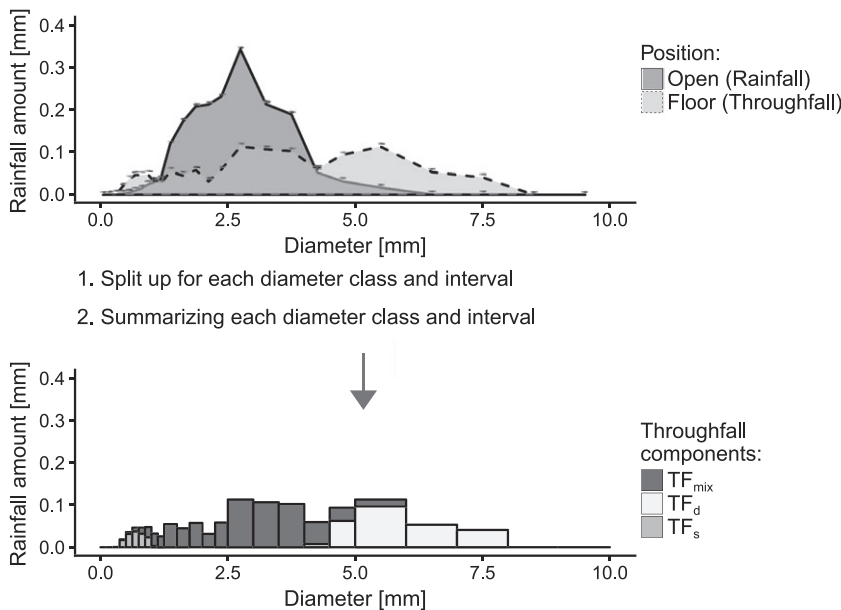


FIGURE 1 Scheme of throughfall fractions separation by subtraction of rainfall (open) and throughfall (floor) spectra. Components are throughfall (TF) with splash droplets (TF_s), TF composed of canopy drip (TF_d), mixed fraction (TF_{mix}), containing free TF, and not distinguishable TF from TF_d or TF_s

Calculation and statistical analyses were done with the statistical language R version 3.3. A linear model with log transformation was used to analyse the relationship between maximum RR and the relative TF components.

2.3 | Definition of rain events

Dunkerley (2008) clearly showed that event parameters highly depend on the initial definition of a rain event. In our study, the following criteria were set to define a rain event: Start and end of an event were at a $RR > 0.001 \text{ mm hr}^{-1}$ (Parsivel detection limit) for a 4-min interval. The minimum drop number threshold was set to >500 drops per event at open rainfall position in order to exclude errors caused by spider webs or other particles. In case of very short events, also diameter-velocity relationship was checked visually to identify uncommon rainfall spectra. In order to classify events and intervals better, these were put into three intensity levels ordered by maximum rain rate (RR_{\max} ; light: $RR_{\max} < 1 \text{ mm hr}^{-1}$, medium: $RR_{\max} 1\text{--}5 \text{ mm hr}^{-1}$, and strong: $RR_{\max} > 5 \text{ mm hr}^{-1}$).

Special care was taken in case of rapid events with different long interruptions, because canopy acts as storage and releases TF during rainfall pauses. These breaks typically showed a significant count of large drops released by the canopy at the floor measurement position and no counts at open rainfall position (tower). The selection was done manually, and events were merged.

3 | RESULTS

3.1 | Observed rain events

A total number of 19 events for beech (eight light, three medium, and eight strong events) and 13 for spruce (four light, seven medium, and two strong events) were observed when both disdrometers were functioning properly (see also Table 1 and Tables A1 and A2). Events at the beech position had an RA ranging from 0.01 to 55.4 mm with a mean RR from 0.03 to 3.79 mm hr^{-1} and event duration ranging from 16 to 2,368 min. For spruce, RA ranged from 0.02 to 6.41 mm with an average RR from 0.04 to 3.17 mm hr^{-1} and event duration ranging from 12 to 876 min, respectively.

The strongest event under beech was event 2 (see appendix Table A1) with a maximum RR of 28.6 mm hr^{-1} within a 4-min interval. Beech event 16 (see Table A1) had an RA of 55 mm with a duration of 2,368 min and a total of 1.5 million individual drops. For spruce, the maximum RR was moderate with 9.7 mm hr^{-1} for event 23. The longest event with the highest RA of 6.4 mm was event 32 (see Table A2), which lasted 876 min. Further information on single-event characteristics can be found in Tables A1 and A2.

3.2 | Canopy influence on DSD on event scale

All 32 events (see Tables A1 and A2 for single-event descriptions) are summarized on the event scale by mean RR, RA, diameter volume percentiles (D10, D50, and D90), and the calculated TF components

(drip, splash, and mix) in Table 1. For storms of all magnitude and intensities, beech produced higher D50 and D90 values than spruce, which can be also seen on average over all events in a higher percentage of TF_d (20.6%) compared with only 3.6% below spruce. On the contrary, spruce produced more TF_s over all events with 1.7% compared with 1.5% for beech, thus showing a lower D10 with 0.45 mm compared with beech with 0.66 mm.

For medium and strong events, the main volumetric part of the rainfall is transferred into higher diameter classes in form of drip from the storage water in the canopy, especially for beech (see also Table 1). This was observed by an increase of TF_d from 2.5% (light events) to 29.9% at medium and 35.2% at strong events, respectively. In case of spruce, TF_d increased only moderately from 2.2% to 2.4% at medium and 10.8% at strong events, respectively. This shift is visualized by D10/D50/D90 for above and TF spectra as seen by a D90 increase from 2.37 to 6.04 mm for beech (2.16 to 4.95 mm for spruce) within the strong event class (see also Table 1 for D10/D50). Both species had a higher TF_s for strong events. Here, the open rain D10 was also higher than the floor D10. During strong events, spruce produced double TF_s with 5.9% compared with beech with 3.3%.

3.3 | Canopy influence on DSD on interval scale

Because each event covers a wide range of RRs, we evaluated the DSD on interval scale for each 4-min interval at the three intensity levels more in detail. Figure 2 shows changes in DSD between rainfall (open) and TF (floor) for each species for different RR classes. The alteration of the DSD for both species is dependent on the RR intensity, as shown by D10/D50/D90. Bimodal peaks of the open rain spectra were caused by the averaging process.

Light RR intervals (beech: $N = 750$; spruce: $N = 497$) in both species downscaled the incident DSD into a reduced and narrowed spectrum, which consisted mainly of TF_{mix} . However, already at light RR a significant part the precipitation was transferred in diameters outside of the incident DSD, which resulted into TF_d . This transfer was more pronounced in beech than in spruce resulting in a stronger shift of D50 from 0.82 to 2.34 mm (spruce 0.74–1.12 mm) and of D90 from 1.18 to 3.19 mm (spruce 1.04–1.69 mm), respectively.

At medium intensity RR (beech: $N = 386$; spruce: $N = 54$), the DSD of beech and spruce started to show a different distribution compared with open rain DSD. In case of beech, the floor DSD became broader and more flattened compared with the open DSD, and diameters greater than the open DSD were recorded. This was observed in an increase of D90 from 1.73 to 6.03 mm resulting in higher TF_d . In case of spruce, the incident DSD was also flattened. Here, intercepted precipitation was now transferred into both diameter directions at the floor DSD, increasing TF volume on low diameter range by decreasing D10 from 0.73 to 0.44 mm with splashing and small droplets (TF_s) and at high diameter range by increasing D90 from 1.81 to 2.00 mm. Both were now lying outside of the open rain DSD.

In rare occurring strong RR intervals ($N = 46$) above 5 mm hr^{-1} , beech floor DSD followed the trend of medium RR observations with a further increase of higher diameter volume share as also seen in

TABLE 1 Summary of attributes of rainfall and throughfall for the 32 events studied above and below two canopies

Sp.	Lvl.	N	Pos.	D10 (mm)	D50 (mm)	D90 (mm)	RR _{max} (mm hr ⁻¹)	RA (mm)	TF _{mix}	TF _d	TF _s
B	L	8	O	0.61 ± 0.02	0.96 ± 0.04	1.42 ± 0.10	0.53 ± 0.09	0.17 ± 0.07	3.2% ± 0.5%	2.5% ± 1.1%	0.1% ± 0.0%
			F	0.56 ± 0.03	2.02 ± 0.59	2.70 ± 0.65	0.09 ± 0.04	0.02 ± 0.01			
	M	3	O	0.64 ± 0.01	1.05 ± 0.02	1.73 ± 0.06	1.85 ± 0.51	0.71 ± 0.14	10.5% ± 3.5%	29.9% ± 13.7%	0.5% ± 0.3%
			F	0.78 ± 0.08	3.41 ± 0.44	5.47 ± 0.44	1.45 ± 0.72	0.34 ± 0.20			
	S	8	O	0.76 ± 0.05	1.35 ± 0.10	2.37 ± 0.18	11.33 ± 2.78	11.74 ± 6.39	27.4% ± 3.2%	35.2% ± 2.8%	3.3% ± 0.6%
			F	0.71 ± 0.01	3.11 ± 0.07	6.04 ± 0.07	7.14 ± 2.38	8.35 ± 4.35			
	All	19	O	0.68 ± 0.03	1.14 ± 0.06	1.87 ± 0.13	5.28 ± 1.66	5.12 ± 2.91	14.6% ± 2.9%	20.6% ± 4.3%	1.5% ± 0.4%
			F	0.66 ± 0.03	2.7 ± 0.28	4.54 ± 0.46	3.27 ± 1.25	3.57 ± 2.01			
Spr	L	4	O	0.49 ± 0.02	0.78 ± 0.05	1.18 ± 0.14	0.35 ± 0.24	0.09 ± 0.11	14.7% ± 3.9%	2.2% ± 2.2%	0.4% ± 0.3%
			F	0.46 ± 0.01	0.72 ± 0.04	1.86 ± 0.86	0.07 ± 0.07	0.02 ± 0.03			
	M	7	O	0.59 ± 0.04	1.02 ± 0.05	1.76 ± 0.08	2.61 ± 1.19	1.46 ± 2.21	12.6% ± 2.3%	2.4% ± 1.8%	1.3% ± 0.5%
			F	0.45 ± 0.02	0.76 ± 0.04	2.11 ± 0.57	0.35 ± 0.33	0.46 ± 1.04			
	S	2	O	0.78 ± 0.08	1.28 ± 0.08	2.16 ± 0.05	8.26 ± 2.05	2.93 ± 1.15	18.3% ± 0.6%	10.8% ± 1.7%	5.9% ± 0.7%
			F	0.46 ± 0.01	1.05 ± 0.01	4.95 ± 0.25	2.38 ± 0.70	1.04 ± 0.48			
	All	13	O	0.59 ± 0.03	0.98 ± 0.06	1.64 ± 0.11	2.79 ± 0.79	1.26 ± 0.52	14.2% ± 1.7%	3.6% ± 1.4%	1.7% ± 0.6%
			F	0.45 ± 0.03	0.80 ± 0.04	2.47 ± 0.48	0.58 ± 0.24	0.41 ± 0.23			

Notes. Attributes comprise mean diameter volume percentiles (D10, D50, and D90 [mm]), precipitation parameters (RA: rain amount [mm], RR: rain rate [mm hr⁻¹]) as well as relative components (mix, splashing, and dripping) of TF percentage of the incoming RA at Pos. O with standard deviation for the three intensity levels (Lvl; light (L): RR_{max} < 1 mm hr⁻¹, medium (M): RR_{max} 1–5 mm hr⁻¹, strong (S): RR_{max} > 5 mm hr⁻¹), and all: all events for the respective species.

Abbreviations: B, beech; F, throughfall measured at floor position; N, number of events; O, open rainfall measured at tower position above canopy; Pos, Position; Sp, species; Spr, spruce.

increases of D50 (1.55–3.13 mm) and D90 (2.47–6.03 mm). For spruce, only a very low number of strong RR intervals ($N = 6$) were observed, but here, a clear shift of the floor DSD towards the lower diameter range could be seen, where floor D50 reached almost the D50 of the open rain position with 0.74 mm compared with 1.34 mm, respectively. This change can be explained by a high TF_d part with D10 of 0.40 mm at floor level and 0.86 mm at open level, respectively. Nevertheless, beech also showed an increase of the TF_s part by D10 change from 0.90 to 0.72 mm at floor level.

The percentage of TF volume completely lying outside the incident spectrum was on average 50.3% for medium and 39.8% for strong events under beech and 8.4% for medium and 2.5% for strong events under spruce, respectively. Beech was able to produce larger drip diameters, but both species had similar peaks around diameter class 5.5 mm at the drip fraction. The spruce DSD was less pronounced in the higher diameter range than beech. A bimodal distribution (one maximum is within the incident spectrum and one in the dripping fraction) could be seen for medium and strong events in Figure 2. This spreading was more pronounced for spruce than for beech.

3.4 | Intraevent development of DSD

The variability of D50 during natural rain events on both measurement positions becomes even more evident, when intraevent processes are analysed (Figures 3 and 4). TF D50 varies with RR and

possible canopy vibration caused by wind as described by Nanko et al. (2006). The DSD development during an event is influenced by several redistribution effects performed by the interception of the canopies.

Figure 3 shows the development of DSD and other rain event parameters for rain event 2 (Table A1) under beech. The event was split into three periods; a first rain subevent lasts about 108 min, followed by about an 84-min rain pause, and another weaker event of 92 min in the third part of the event. Specific event parameters of each period are listed in Table 2.

During this event, DSD considerably changed under the canopy at floor position:

In the first 16 min (0.27 mm of incident RA), only a small range of drops reached the surface in a reduced spectrum (floor RA of 0.01 mm). D10, D50, and D90 were smaller than the open rainfall spectrum. Afterwards, the TF DSD changed at several time points; due to the intensification of the event to an RR of 28 mm hr⁻¹ after 20 min and 23 mm hr⁻¹ after 24 min, the canopy storage capacity was probably reached and started to drip, resulting in higher D50 and D90 values. At both maxima, the impacting drops on the canopy split into splashing droplets resulting into 220% and 253% more TF drops compared with open rainfall (panel 3 of Figure 3), respectively. Consequently, the TF D10 values were lower than the rainfall D10, because of a high amount of small droplets in these lower diameters.

During rain, pause drops accumulated previously were still dripping to the surface in form of canopy drip, but their number of 30 ±

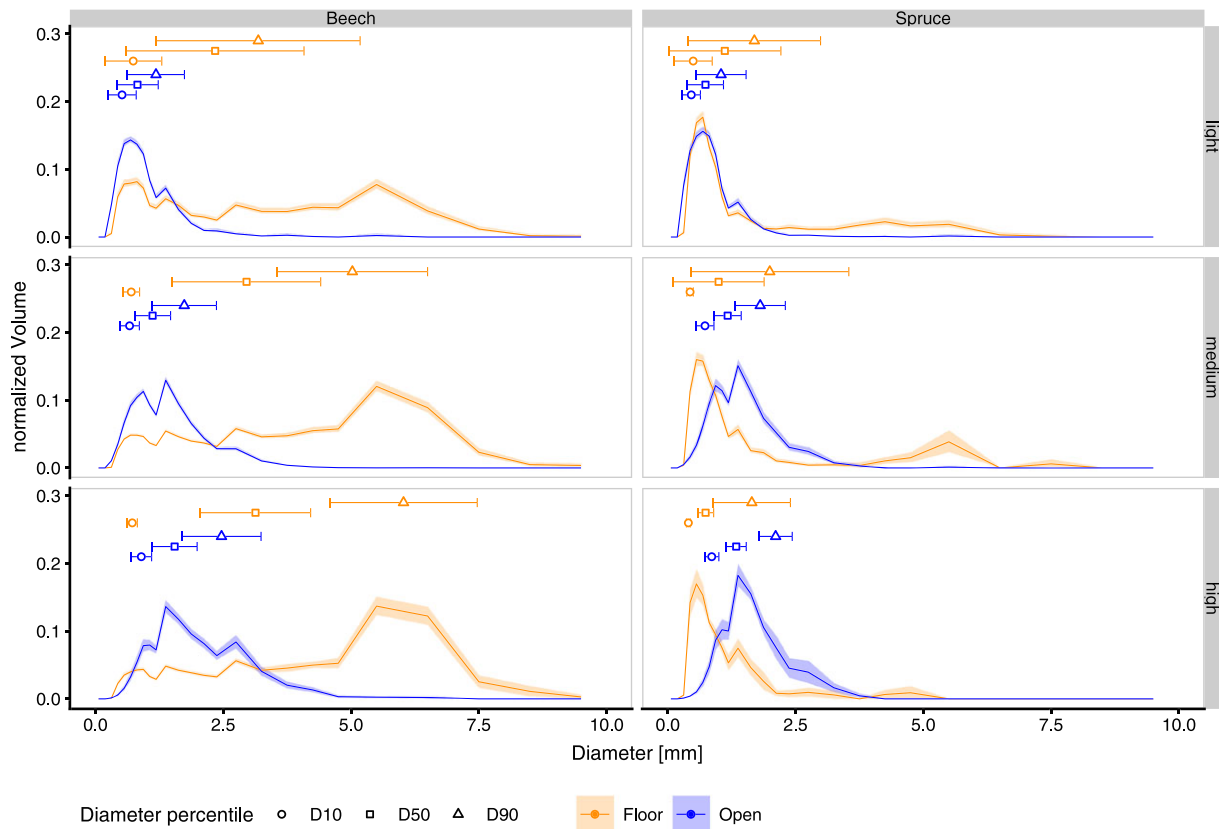


FIGURE 2 Drop size distribution of mean normalized rain amount in rainfall (open) and throughfall (floor) measurements for the three intensity classes and two canopy species beech and spruce at a 4-min interval scale. Intensity levels (RR_{max} , maximum rainfall rates) are defined by light: $RR_{max} < 1 \text{ mm hr}^{-1}$, medium: $RR_{max} 1\text{--}5 \text{ mm hr}^{-1}$, strong: $RR_{max} > 5 \text{ mm hr}^{-1}$. Transparent area represents the standard error. Points represent three volume percentile marks D10, D50, and D90 at 10%/50%/90% with their standard error shown by error bars

4 drops per interval was low compared with a mean drop number of $1,470 \pm 503$ at the first and 278 ± 58 in the third subevent period. Their drop size was also reduced as seen in the TF D10, D50, and D90 (see Table 2).

The third period showed a fast rise of the TF spectrum with increasing RR similar to the first subevent. However, RR and RA were five times lower. D50 at both sites were lower in the third period, but still there was an approximately 2.5 times higher TF D50 (Figure 3, Table 2).

Figure 4 shows the variability of the spectrum for spruce in a strong rain event. This event 23 (appendix Table A2) was one of the two strong events recorded under spruce. It was characterized by a maximum RR of 9.7 mm hr^{-1} and a total RA of 2.1 mm (Figure 4 panel 2) and, thus, was much shorter and less intensive than the comparable beech event (Figure 3). However, several aspects in the development of the DSD have to be discussed. The RR maximum with 9.7 mm hr^{-1} occurred in the interval after 16 min and declined to 6 mm hr^{-1} after 28 min. During this phase, splashing was clearly visible in the TF part due to lower D10 ranging from 0.37 to 0.48 mm (1.13 to 0.78 mm at rainfall D10) and about 30% to 50% more drops than in incident rainfall.

After 24 minutes, droplet size tended to increase with a higher D50 value of 4.2 mm, D90 of 5.2 mm, and a higher TF RR. However,

the main amount of dripping was primarily falling during the interval at 28 min, because the following intervals (until minute 40) were showing only a marginal increase of the TF cumulative RA.

3.5 | Factors controlling TF partitioning

For each event, the intensity classification was done based on the maximum RR occurring within the event. Figure 5 presents a regression of the logarithm of RR with each fraction.

Beech showed significant regressions with a good coefficient of determination for all TF components, whereas for spruce most regressions were not significant.

For beech, the decrease of the DIFF component coincided with the increase of the other fractions, because fewer amounts were intercepted. TF fractions TF_{mix} and TF_d were moving identically towards a limit. TF_s increased only slowly on RR_{max} and seemed also to move against a certain limit as seen in Figure 5.

For beech, all fractions were highly significant and only differed in their relevance. TF_{mix} and DIFF with a R^2 of 0.79 and 0.73 had a high relevance (Table 3). Both are highly dependent on the RR. TF_s and TF_d had lower R^2 of 0.67 and 0.57 than DIFF and TF_{mix} and were not significantly depending on RR (Table 3). With increasing RR, all components seem to approach asymptotically a limit.

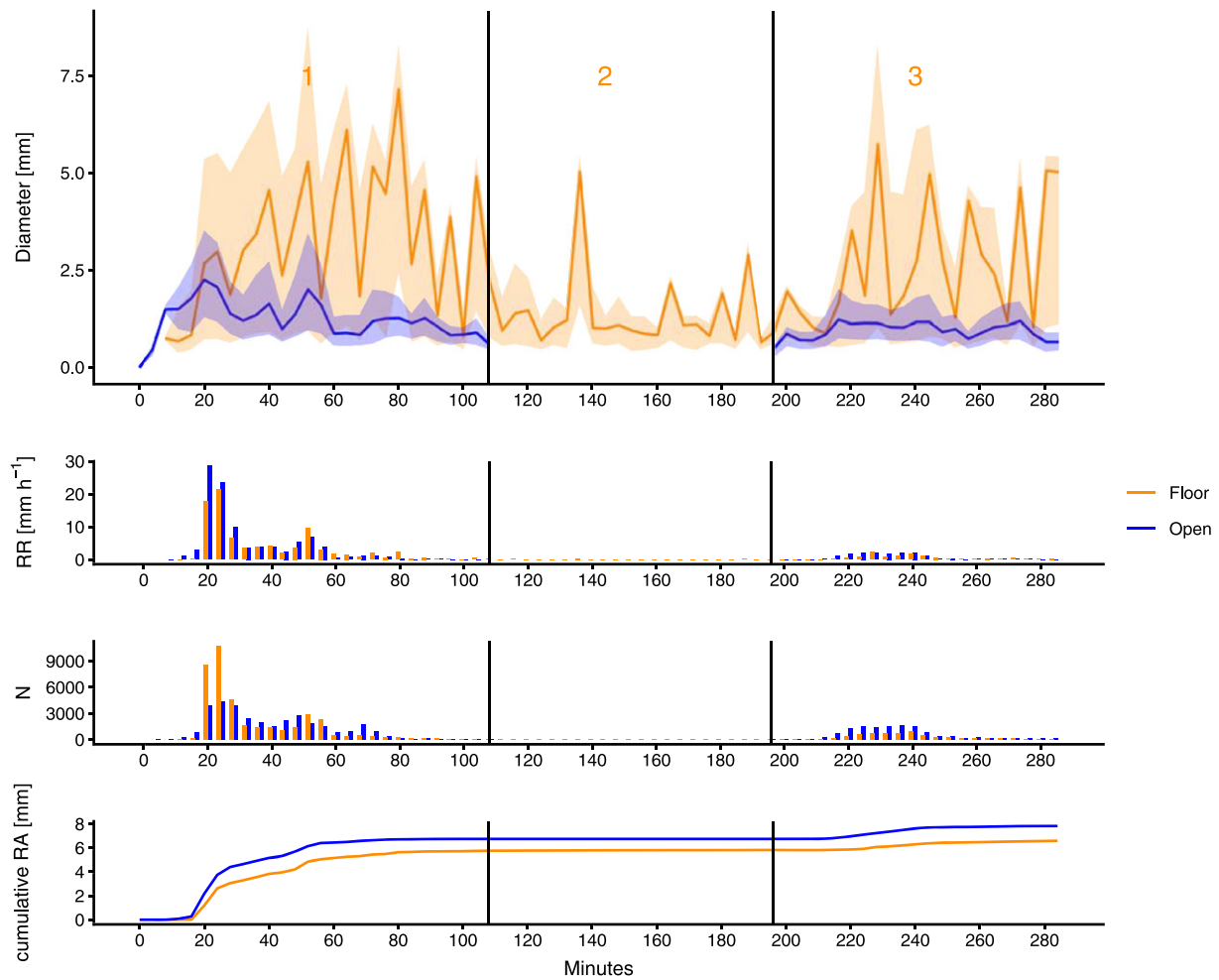


FIGURE 3 Intraevent variation of drop size distribution parameters during event 2 for beech and its three subevent periods at open and floor measurement position (see also Table 2). (Top panel) diameter volume percentiles (D10/D50/D90) for 4-min intervals. The semitransparent areas are ranging from D10 to D90, and the middle line represents the D50 value. The lower three panels show further rainfall parameters: (Second panel) rain rate (RR: mm hr⁻¹) for 4-min intervals; (Third panel) current number of drops per 4-min interval; (bottom panel) cumulative rain amount during the total event. Please note different scaling on the y-axis. First rainfall record is after 4 min (first record interval). See also Figure A1 for an enlarged part of subevent 2

For spruce, the total range of event intensities is too small to give general answers on the dependencies of these fractions on RR. A longer period of measurements with a broader range of intensity types would be necessary. Only TF_s was significant and showed a good dependence on RR_{max} with $R^2 = 0.54$. For TF_d , the significance level was low, but RR_{max} had a low relevance of $R^2 = 0.29$. In case of $DIFF$ and TF_{mix} , the R^2 was low with 0.18 and 0.01, respectively. Both were not significant.

4 | DISCUSSION

4.1 | DSD change in relation to canopy influence

The DSD change (Figures 2–4) engendered by the interaction of incoming rainfall with canopies resulted in a wider diameter range for intense events and a narrower diameter range for lower intensity events for both tree species. Redistribution into other diameter

classes was observed for all intensities, however, most visible at intense events. The origin of drop diameters lying outside the incident DSD could be considered to come from accumulated intercepted drops on the canopy surface (Vis, 1986). Reaching a species-specific storage capacity of the leaves or other canopy surfaces results in the formation of canopy drip for several tree species (e.g., Xiao & McPherson, 2016). Higher amounts at lower diameter sizes could be related to impact or splashing droplets from collision of drops with the plant surface (e.g., Herwitz, 1987; Yang & Madden, 1993) or with each other (McTaggart-Cowan & List, 1975). Another source of small droplets results from drops, which break due to their unstable large size (McTaggart-Cowan & List, 1975), which can happen at this site because distance between floor and lowest branches is about 12 to 18 m, and drops can accelerate to terminal velocity

When comparing our normalized TF and rainfall DSD (Figure 2) with that of Hall and Calder (1993) and Nanko et al. (2006), we find similar changes in the DSD in form of an increase in higher diameter

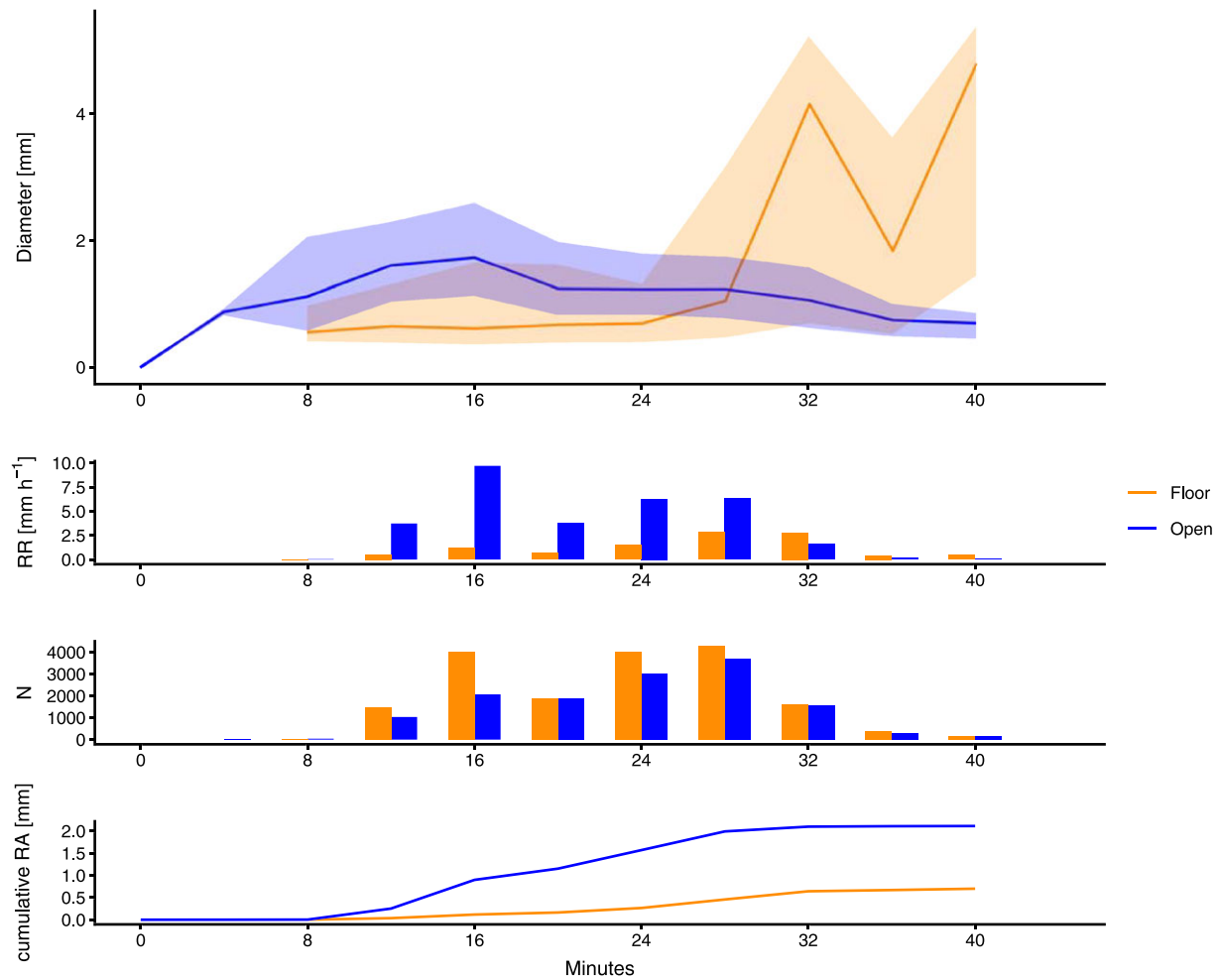


FIGURE 4 Intraevent variation drop size distribution parameters during event 23 under spruce for a 4-min interval at open and floor measurement position. (Top panel) diameter volume percentiles (D10/D50/D90) for 4-min intervals. The semitransparent areas are ranging from D10 to D90, and the middle line represents the D50 value. The lower three panels show further rainfall parameters: (Second panel) rain rate (RR: mm hr⁻¹) for 4-min intervals; (Third panel) current number of drops per 4-min interval; (bottom panel) cumulative rain amount during the total event. Please note different scaling on the y-axis. First rainfall record is after 4 min (first record interval)

TABLE 2 Specific drop size distribution characteristics for three subevent periods of event 2 for beech (see also Table A1)

No.	Duration (min.)	Pos.	RA (mm)	N	N_{mean} per interval	RR_{mean} (mm hr ⁻¹)	RR_{max} (mm hr ⁻¹)	D10 (mm)	D50 (mm)	D90 (mm)
1	108	O	6.75	33,459	1,239	3.893	28.6	0.78	1.26	1.89
		F	5.75	39,708	1,470	3.323	21.4	0.84	3.20	4.87
2	84	O	0.00	0	0	0.000	0.0	0.00	0.00	0.00
		F	0.06	631	30	0.040	0.3	0.61	1.38	1.84
3	92	O	1.08	13,187	551	0.674	2.1	0.60	0.95	1.35
		F	0.78	6,407	278	0.492	2.4	0.71	2.62	3.79

Abbreviations: D10, 10th percentile volume diameter (mm); D50, median volume diameter (mm); D90, 90th percentile volume diameter (mm) at each position of the disdrometer (O, rainfall measured at open tower position; F, throughfall measured at floor position); N, number of drops; N_{mean} , number of drops per 4-min interval; RA, rain amount (mm); RR_{max} , maximum rain rate (mm hr⁻¹); RR_{mean} , mean rain rate (mm hr⁻¹).

sizes and reduction in the area of the incident open rain DSD. In terms of species, differences were also apparent. Spruce tended to produce smaller drip, and their main amount was lower than under broadleaved species. However, we measured that TF under spruce at high RA and RR could also drip in larger drops, probably because the

needles on the twigs could be connected in larger water films resulting in larger water storage for larger drop diameters as observed by Nanko et al. (2013) for example. Compared with spruce, beech produced large drops, even at low rain rates, due to the large surface area (see also methods, Reiter et al., 2005) and a higher leaf density

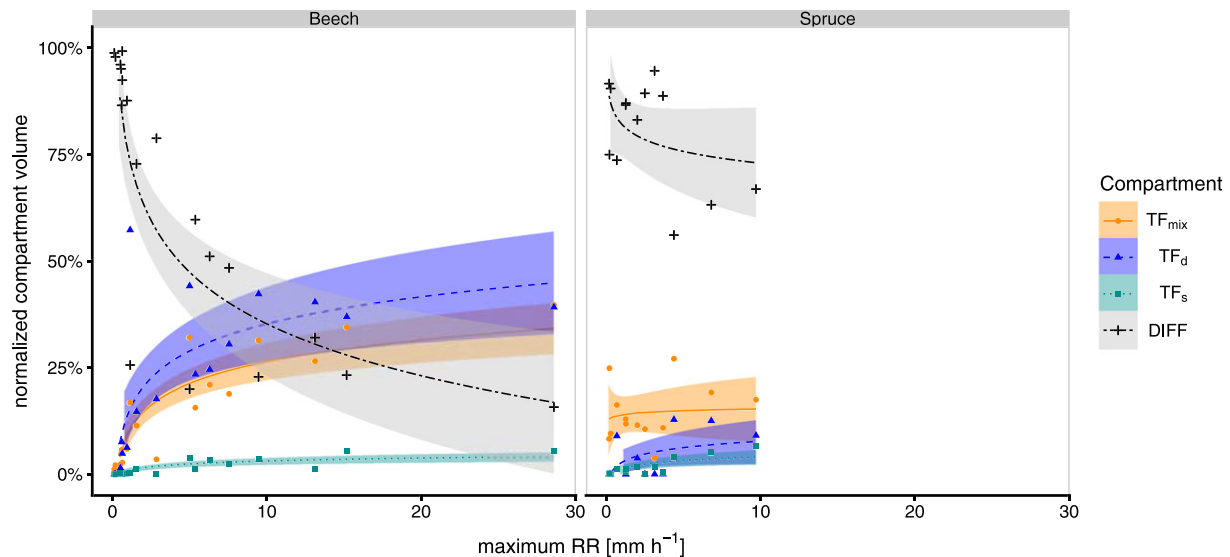


FIGURE 5 Log-linear regression model on the normalized components volume (scaled on incoming rainfall) and the maximum rain rate in mm hr^{-1} for spruce and beech. Components are throughfall (TF) with splash droplets (TF_s), TF composed of canopy drip (TF_d), mixed fraction TF_{mix} , containing free TF, and not distinguishable TF from TF_d or TF_s , and the difference between rainfall and total throughfall (DIFF)

TABLE 3 Regression parameters of Figure 5

Fraction	Species	p	Equation		R^2
			Intercept	$\log(\text{RR}_{\text{max}})$	
DIFF	B	<.001	0.756	−0.175	0.734
	Spr	.153	0.821	−0.04	0.176
TF_d	B	<.001	0.142	0.092	0.565
	Spr	.059	0.027	0.022	0.287
TF_s	B	<.001	0.008	0.01	0.670
	Spr	.004	0.012	0.012	0.543
TF_{mix}	B	<.001	0.094	0.074	0.789
	Spr	.70	0.139	0.006	0.014

Notes. Components are TF with splash droplets (TF_s), TF composed of canopy drip (TF_d), TF_{mix} , containing free TF, not distinguishable from TF_d or TF_s , and difference between rainfall and total throughfall (DIFF).

(Häberle et al., 2003), which could intercept drops better and generate a larger storage to form large drops.

4.2 | D50, D10, and D90 for different species and event types

Several parameters are dependent on the canopy species; thus, TF D50 (see Tables A1 and A2) with a sample size above 10,000 drops per event was investigated to compare this parameter for higher RR with the D50 reported by Hall and Calder (1993) and Nanko et al. (2006). The D50 under spruce ranged from 1.29 to 1.76 mm in our study. D50 of spruce was lower than the other needle-leaved species measured by Nanko et al. (2006) ranging from 2.14 to 2.87 mm and Hall and Calder (1993) with 2.3 mm. It was, however, much lower than the D50 of 4.4 mm measured by Armstrong and Mitchell (1987),

which was done by dye paper at short-time intervals and thus relative low sample number.

The D50 of beech from 2.46 to 2.98 mm was comparable with the D50 of 2.50 mm at 60% leaf cover under beech measured by Trucchi and Andrenelli (2007). It also lies around that of broadleaved species as measured by Nanko et al. (2006) with 2.77 mm and between both species of Hall and Calder (1993) ranging from 2.8 to 4.2 mm. The different ranges show that specific leaf and canopy characteristics (see, e.g., Hall & Calder, 1993; Nanko et al., 2006; Nanko et al., 2013) such as surface properties, shape, and surface area affect D50. In regard to meteorological factors, maximum RR increased the TF D50 in our study to some extent. But also other meteorological parameters, such as wind speed and temperature, influenced the TF D50 as shown by Nanko et al. (2016).

Our analysis and the one by Nanko et al. (2006) showed similar results, and unlike Brandt (1989) who stated that TF DSD is neither

influenced by species or RR, both showed a major role in TF D50. However, former procedures for drop size measurements were mainly manual and had lower sample sizes. This is especially true for lower intensity events, because for events with lower drop numbers, the D50 values had higher variability, and one large diameter drop represents a high percentage of the whole RA as shown in Figures 3 and 4.

A closer look on event developments (Figures 3 and 4) shows that TF D50 became larger than the rainfall D50 if a specific cumulative RA stored in the canopy was reached, which was difficult to quantify, because it is dependent on meteorological factors (e.g., wind and temperature; Nanko et al., 2016) and the canopy structure above the disdrometer (Frasson & Krajewski, 2011). The behaviour of D10 values under spruce (Figure 5) showed that when TF D10 is lower than rainfall D10, a high amount of splashing with a large number of small droplets occurred. In the same event, the TF D50 was even smaller than the rainfall D10, which means that 50% of the TF RA lay below the diameter of 10% volume of incoming rainfall (Figure 5).

4.3 | TF fractions

We propose a method to split up the TF into three components: TF_d , TF_s , and TF_{mix} , representing the different redistributed amounts under the canopy. These would generally be referred to Dunkerley (2000) as release TF (TF_d and TF_s) and direct or free TF (most part of TF_{mix}). Normally, free and release TF is measured as a whole with rain gauges or funnel gauges, which makes partitioning into fractions/components impossible.

Yet, the results of the partitioning represent only one specific floor location below the canopy, and thus, the high spatial variability of TF under the canopy (Levia & Frost, 2006) was not considered. Experimentally, Nanko, Onda, Ito, and Moriwaki (2011) showed a high spatial variability under the crown of a Japanese cypress, depending on the branch and leaf density and geometry. Because disdrometers currently are more expensive than rain gauges and accumulation over an area by a funnel is technically not possible (see above), a wide scale measurement of TF fractions requires a higher number of devices and, thus, investment costs. Another option to resolve this problem would be a moveable device, but position could only change between the events because otherwise the variability within the event and the variability between each position are not separable from each other.

The PARSIVEL also measures the drop velocity; thus, these properties should be included for separating free TF from release TF and the assumed falling height of drops as previously shown by Wakiyama et al. (2010) and Nanko et al. (2011). Through placing the disdrometer higher and closer to the lower canopy edge, velocity differences between the incident and new drops should be visible, which then support this novel approach for TF partitioning. For low canopies such as maize, this approach was shown by a study of Frasson and Krajewski (2011) in which direct and indirect TF were detected with a disdrometer.

For the whole event, the TF components were reasonably linked to event intensity (Figure 5), where TF_d and TF_{mix} were increasing, and DIFF was decreasing for beech with increasing intensity. For

spruce, the number of events and their intensities were too low to definitively assess these relationships. Further, the selected below canopy floor position could be problematic (see Nanko et al., 2011), because spruce transports water into the border of the conical-shaped crown. The development of each component amount could be explained by the storage models (e.g., Rutter, Kershaw, Robins, & Morton, 1971; Rutter, Morton, & Robins, 1975), where intercepted precipitation can either evaporate, run off the stem, or drip from the different canopy surfaces. As seen in Figure 5, DIFF was asymptotically approaching a specific threshold; on very long events with constant precipitation input, the DIFF would probably be near a limit only consisting of stemflow.

4.4 | Wider implications

This study sought to fill an existing data gap on the effects of European beech and Norway spruce, two major European tree species, on TF DSD in relation to contrasting canopy structures. The mean \pm standard deviation of the median volume drops size (D50) over all rain events was 2.7 ± 0.28 mm for beech and 0.80 ± 0.04 mm for spruce, respectively. Moreover, the maximum drop sizes under beech were higher than under spruce. Given the significant differences in TF partitioning between European beech and Norway spruce, we make a call for studies that link TF types to soil moisture levels, soil respiration, and nitrous oxide emissions from forest soils. Such work would improve our knowledge as to how different types of TF affect (and may induce) fine scale hot spots in soil-atmosphere interactions as well as biogeochemical cycling in forests.

5 | CONCLUSION

This study showed that the contrasting canopy structures of European beech and Norway spruce have a substantial and differential influence on TF DSD. Specifically, beech and spruce showed a clear difference between their diameter volume percentiles. This means that the canopy and leaf structure of major European species lead to a different width of TF spectra, which is generally wider for beech and more narrow for spruce. The width of the spectra and therefore the contribution each TF type is dependent on both tree species and rain event characteristics.

We separated the TF into three classes: TF_d , TF_s , and TF_{mix} using literature-based thresholds. TF_{mix} is compromised to incorporate the uncertainty in determining splash and drip droplets within the diameter range from 1 to 2 mm. Additionally, this class includes direct TF as well as other unknown contributions. TF_d consists of lower number large droplets released by the canopy and is deepened on the stored water in canopy and RR. It represents a larger fraction the total TF. TF_s contains many small droplets (<1 mm) created by impacts on the canopy. However, it is only representing a small percentage of the total TF, increasing during intense events.

Together with TF_{mix} , all TF components allow a more detailed view on temporal distribution and the influence of the canopy itself.

However, for improving the fraction measurements, several things should be done:

More precipitation event types should be measured to gather more information on the dependencies of TF components. Using more disdrometers below the canopy will reduce the effect of spatial variability. Stemflow needs to be assessed to cover the whole of net precipitation partitioning and determine interception. However, more information on canopy/forest structure also is required to improve process understanding and create suitable models. Tools such as laser-based 3-D scanners or photogrammetry by UAV/cameras allow fast determination of 3-D forest structures. Also, more canopy species should be observed in parallel to get information on influence parameters, which are driven by the canopy structure.

ACKNOWLEDGMENT

Thanks to Dr. H. Franz of the Berchtesgaden National Park for lending us the second disdrometer.

CONFLICT OF INTEREST

No conflict of interest.

DATA AVAILABILITY STATEMENT

Data available on request from the authors.

ORCID

Marvin Lüpke  <https://orcid.org/0000-0002-5045-134X>

Delphis Levia  <https://orcid.org/0000-0002-7443-6523>

Kazuki Nanko  <https://orcid.org/0000-0002-1157-9287>

REFERENCES

- Armstrong, C. L., & Mitchell, J. K. (1987). Transformations of rainfall by plant canopy. *Transactions of ASAE*, 30(3), 688–696. <https://doi.org/10.13031/2013.3046>
- Battaglia, A., Rustemeier, E., Tokay, A., Blahak, U., & Simmer, C. (2010). PARSIVEL Snow observations: A critical assessment. *Journal of Atmospheric and Oceanic Technology*, 27(2), 333–344. <https://doi.org/10.1175/2009JTECHA1332.1>
- Bentley, W. (1904). Studies of raindrops and raindrop phenomena. *Monthly Weather Review*, 32(10), 450–456.
- Brandt, C. J. (1989). The size distribution of throughfall drops under vegetation canopies. *Catena*, 16(4–5), 507–524. [https://doi.org/10.1016/0341-8162\(89\)90032-5](https://doi.org/10.1016/0341-8162(89)90032-5)
- Chapman, G. (1948). Size of raindrops and their striking force at the soil surface in a red pine plantation. *Transactions of the American Geophysical Union*, 29(5), 664. <https://doi.org/10.1029/TR029i005p00664>
- Crockford, R. H., & Richardson, D. P. (2000). Partitioning of rainfall into throughfall, stemflow and interception: Effect of forest type, ground cover and climate. *Hydrological Processes*, 14(16–17), 2903–2920. [https://doi.org/10.1002/1099-1085\(200011/12\)14:16/17<2903::AID-HYP126>3.0.CO;2-6](https://doi.org/10.1002/1099-1085(200011/12)14:16/17<2903::AID-HYP126>3.0.CO;2-6)
- Davidson, E. A., Ishida, F. Y., & Nepstad, D. C. (2004). Effects of an experimental drought on soil emissions of carbon dioxide, methane, nitrous oxide, and nitric oxide in a moist tropical forest. *Global Change Biology*, 10(5), 718–730. <https://doi.org/10.1111/j.1365-2486.2004.00762.x>
- Dunkerley, D. (2000). Measuring interception loss and canopy storage in dryland vegetation: A brief review and evaluation of available research strategies. *Hydrological Processes*, 14(4), 669–678. [https://doi.org/10.1002/\(SICI\)1099-1085\(200003\)14:4<669::AID-HYP965>3.0.CO;2-I](https://doi.org/10.1002/(SICI)1099-1085(200003)14:4<669::AID-HYP965>3.0.CO;2-I)
- Dunkerley, D. (2008). Rain event properties in nature and in rainfall simulation experiments: A comparative review with recommendations for increasingly systematic study and reporting. *Hydrological Processes*, 22(22), 4415–4435. <https://doi.org/10.1002/hyp.7045>
- Fernández-Raga, M., Fraile, R., Keizer, J. J., Varela Teijeiro, M. E., Castro, A., Palencia, C., ... da Costa Marques, R. L. (2010). The kinetic energy of rain measured with an optical disdrometer: An application to splash erosion. *Atmospheric Research*, 96(2–3), 225–240. <https://doi.org/10.1016/j.atmosres.2009.07.01>
- Frasson, R. P. D. M., & Krajewski, W. F. (2011). Characterization of the drop-size distribution and velocity-diameter relation of the throughfall under the maize canopy. *Agricultural and Forest Meteorology*, 151(9), 1244–1251. <https://doi.org/10.1016/j.agrformet.2011.05.001>
- Gunn, R., & Kinzer, G. D. (1949). The terminal velocity of fall for water droplets in stagnant air. *Journal of Meteorology*, 6(4), 243–248. [https://doi.org/10.1175/1520-0469\(1949\)006<0243:TTVOFF>2.0.CO;2](https://doi.org/10.1175/1520-0469(1949)006<0243:TTVOFF>2.0.CO;2)
- Häberle, K. H., Reiter, I. M., Nunn, A., Gruppe, A., Simon, U., & Gossner, M. (2003). KROCO, Freising, Germany: Canopy research in a temperate mixed forest of Southern Germany. In Y. Basset, V. Horlyck, & S. J. Wright (Eds.), *Studying forest canopies from above. The International Canopy Crane Network*. Balboa, Ancon, Panama: Smithsonian Tropical Research Institute; UNEP.
- Hall, R. L., & Calder, I. R. (1993). Drop size modification by forest canopies: Measurements using a disdrometer. *Journal of Geophysical Research-Atmospheres*, 98(D10), 18465–18470. <https://doi.org/10.1029/93JD0149>
- Hervitz, S. R. (1987). Raindrop impact and water flow on the vegetative surfaces of trees and the effects on stemflow and throughfall generation. *Earth Surface Processes and Landforms*, 12(4), 425–432. <https://doi.org/10.1002/esp.3290120408>
- Kuptz, D., Matyssek, R., & Grams, T. E. E. (2011). Seasonal dynamics in the stable carbon isotope composition ($\delta^{13}C$) from non-leafy branch, trunk and coarse root CO₂ efflux of adult deciduous (*Fagus sylvatica*) and evergreen (*Picea abies*) trees. *Plant, Cell & Environment*, 34(3), 363–373. <https://doi.org/10.1111/j.1365-3040.2010.02246.x>
- L'Ecuyer, T. S., Kummerow, C., & Berg, W. (2004). Toward a global map of raindrop size distributions. Part I: rain-type classification and its implications for validating global rainfall products. *Journal of Hydrometeorology*, 5(5), 831–849. [https://doi.org/10.1175/1525-7541\(2004\)005<0831:TAGMOR>2.0.CO;2](https://doi.org/10.1175/1525-7541(2004)005<0831:TAGMOR>2.0.CO;2)
- Levia, D. F., & Frost, E. E. (2006). Variability of throughfall volume and solute inputs in wooded ecosystems. *Progress in Physical Geography: Earth and Environment*, 30(5), 605–632. <https://doi.org/10.1177/0309133306071145>
- Levia, D. F., Hudson, S. A., Llorens, P., & Nanko, K. (2017). Throughfall drop size distributions: A review and prospectus for future research. *Wiley Interdisciplinary Reviews Water*, 4(4), e1225. <https://doi.org/10.1002/wat2.1225>
- Levia, D. F., Nanko, K., Amasaki, H., Giambelluca, T. W., Hotta, N., Iida, S., ... Sun, X. (2019). Throughfall partitioning by trees. *Hydrological Processes*, 33(12), 1698–1708. <https://doi.org/10.1002/hyp.13432>
- Liu, Y., Liu, S., Wan, S., Wang, J., Luan, J., & Wang, H. (2016). Differential responses of soil respiration to soil warming and experimental throughfall reduction in a transitional oak forest in central China. *Agricultural and Forest Meteorology*, 226–227, 186–198. <https://doi.org/10.1016/j.agrformet.2016.06.003>

- Löffler-Mang, M., & Joss, J. (2000). An optical disdrometer for measuring size and velocity of hydrometeors. *Journal of Atmospheric and Oceanic Technology*, 17(2), 130–139. [https://doi.org/10.1175/1520-0426\(2000\)017<0130:AODFMS>2.0.CO;2](https://doi.org/10.1175/1520-0426(2000)017<0130:AODFMS>2.0.CO;2)
- Marshall, J. S., & Palmer, W. M. K. (1948). The distribution of raindrops with size. *Journal of Meteorology*, 5(4), 165–166. [https://doi.org/10.1175/1520-0469\(1948\)005](https://doi.org/10.1175/1520-0469(1948)005)
- McTaggart-Cowan, J. D., & List, R. (1975). Collision and breakup of water drops at terminal velocity. *Journal of the Atmospheric Sciences*, 32(7), 1401–1411. [https://doi.org/10.1175/1520-0469\(1975\)032%3C1401:CABOWD%3E2.0.CO](https://doi.org/10.1175/1520-0469(1975)032%3C1401:CABOWD%3E2.0.CO)
- Mosley, M. P. (1982). The effect of a new zealand beech forest canopy on the kinetic energy of water drops and on surface erosion. *Earth Surface Processes and Landforms*, 7(2), 103–107. <https://doi.org/10.1002/esp.3290070204>
- Moss, A. J., & Green, T. W. (1987). Erosive effects of the large water drops (gravity drops) that fall from plants. *Soil Research*, 25(1), 9. <https://doi.org/10.1071/SR9870009>
- Nanko, K., Hotta, N., & Suzuki, M. (2004). Assessing raindrop impact energy at the forest floor in a mature Japanese cypress plantation using continuous raindrop-sizing instruments. *Journal of Forest Research*, 9(2), 157–164. <https://doi.org/10.1007/s10310-003-0067-6>
- Nanko, K., Hotta, N., & Suzuki, M. (2006). Evaluating the influence of canopy species and meteorological factors on throughfall drop size distribution. *Journal of Hydrology*, 329(3–4), 422–431. <https://doi.org/10.1016/j.jhydrol.2006.02.03>
- Nanko, K., Hudson, S. A., & Levía, D. F. (2016). Differences in throughfall drop size distributions in the presence and absence of foliage. *Hydrological Sciences Journal*, 61(3), 620–627. <https://doi.org/10.1080/02626667.2015.1052454>
- Nanko, K., Onda, Y., Ito, A., & Moriwaki, H. (2011). Spatial variability of throughfall under a single tree: Experimental study of rainfall amount, raindrops, and kinetic energy. *Agricultural and Forest Meteorology*, 151(9), 1173–1182. <https://doi.org/10.1016/j.agrformet.2011.04.006>
- Nanko, K., Watanabe, A., Hotta, N., & Suzuki, M. (2013). Physical interpretation of the difference in drop size distributions of leaf drips among tree species. *Agricultural and Forest Meteorology*, 169, 74–84. <https://doi.org/10.1016/j.agrformet.2012.09.018>
- Ovington, J. D. (1954). A comparison of rainfall in different woodlands. *Forestry*, 27(1), 41–53. <https://doi.org/10.1093/forestry/27.1.41>
- Pretzsch, H., Rötzer, T., Matyssek, R., Grams, T. E. E., Häberle, K.-H., Pritsch, K., ... Munch, J. C. (2014). Mixed Norway spruce (*Picea abies* [L.] Karst) and European beech (*Fagus sylvatica* [L.] Karst) stands under drought: From reaction pattern to mechanism. *Trees*, 28(5), 1305–1321. <https://doi.org/10.1007/s00468-014-1035-9>
- Raupach, T. H., & Berne, A. (2015). Correction of raindrop size distributions measured by Parsivel disdrometers, using a two-dimensional video disdrometer as a reference. *Atmospheric Measurement Techniques*, 8(1), 343–365. <https://doi.org/10.5194/amt-8-343-2015>
- Reiter, I. M. (2004). Space-related resource investments and gains of adult beech (*Fagus sylvatica*) and spruce (*Picea abies*) as a quantification of aboveground competitiveness. PhD-Thesis. München, Freising.
- Reiter, I. M., Häberle, K.-H., Nunn, A. J., Heerdt, C., Reitmayer, H., Grote, R., & Matyssek, R. (2005). Competitive strategies in adult beech and spruce: Space-related foliar carbon investment versus carbon gain. *Oecologia*, 146(3), 337–349. <https://doi.org/10.1007/s00442-005-0146-9>
- Rutter, A. J., Kershaw, K. A., Robins, P. C., & Morton, A. J. (1971). A predictive model of rainfall interception in forests, 1. Derivation of the model from observations in a plantation of Corsican pine. *Agricultural Meteorology*, 9, 367–384. [https://doi.org/10.1016/0002-1571\(71\)90034](https://doi.org/10.1016/0002-1571(71)90034)
- Rutter, A. J., Morton, A. J., & Robins, P. C. (1975). A predictive model of rainfall interception in forests. II. Generalization of the model and comparison with observations in some coniferous and hardwood stands. *The Journal of Applied Ecology*, 12(1), 367. <https://doi.org/10.2307/240173>
- Salles, C., Poesen, J., & Borselli, L. (1999). Measurement of simulated drop size distribution with an optical spectro pluviometer: Sample size considerations. *Earth Surface Processes and Landforms*, 24(6), 545–556. [https://doi.org/10.1002/\(SICI\)1096-9837\(199906\)24:6<545::AID-ESP3>3.0.CO;2-D](https://doi.org/10.1002/(SICI)1096-9837(199906)24:6<545::AID-ESP3>3.0.CO;2-D)
- Sempere-Torres, D., Porrà, J. M., & Creutin, J.-D. (1998). Experimental evidence of a general description for raindrop size distribution properties. *Journal of Geophysical Research-Atmospheres*, 103(D2), 1785–1797. <https://doi.org/10.1029/97JD02065>
- Shinohara, Y., Ichinose, K., Morimoto, M., Kubota, T., & Nanko, K. (2018). Factors influencing the erosivity indices of raindrops in Japanese cypress plantations. *Catena*, 171, 54–61. <https://doi.org/10.1016/j.catena.2018.06.030>
- Trucchi, P., & Andrenelli, M. C. (2007). Beech coppice leaf cover and gross rainfall qualitative-quantitative transformation in simulated rainfall events of high intensity. In A. Stokes, I. Spanos, J. E. Norris, & E. Cammeraat (Eds.), *Developments in plant and soil sciences. Eco-and ground bio-engineering: The use of vegetation to improve slope stability* (pp. 329–336). Dordrecht: Springer Netherlands.
- Upton, G., & Brown, D. (2008). *An investigation of factors affecting the accuracy of Thies disdrometers*. St. Petersburg: Russian Federation.
- Vis, M. (1986). Interception, drop size distributions and rainfall kinetic energy in four colombian forest ecosystems. *Earth Surface Processes and Landforms*, 11(6), 591–603. <https://doi.org/10.1002/esp.3290110603>
- Wakiyama, Y., Onda, Y., Nanko, K., Mizugaki, S., Kim, Y., Kitahara, H., & Ono, H. (2010). Estimation of temporal variation in splash detachment in two Japanese cypress plantations of contrasting age. *Earth Surface Processes and Landforms*, 35(9), 993–1005. <https://doi.org/10.1002/esp.1844>
- Wipfler, P., Seifert, T., Heerdt, C., Werner, H., & Pretzsch, H. (2005). Growth of adult Norway spruce (*Picea abies* [L.] Karst.) and European beech (*Fagus sylvatica* L.) under free-air ozone fumigation. *Plant Biology*, 7(6), 611–618. <https://doi.org/10.1055/s-2005-872871>
- Xiao, Q., & McPherson, E. G. (2016). Surface water storage capacity of twenty tree species in Davis, California. *Journal of Environmental Quality*, 45(1), 188. <https://doi.org/10.2134/jeq2015.02.0092>
- Yang, X., & Madden, L. V. (1993). Effect of ground cover, rain intensity and strawberry plants on splash of simulated raindrops. *Agricultural and Forest Meteorology*, 65(1–2), 1–20. [https://doi.org/10.1016/0168-1923\(93\)90035-G](https://doi.org/10.1016/0168-1923(93)90035-G)
- Zabret, K., Rakovec, J., Mikoš, M., & Šraj, M. (2017). Influence of raindrop size distribution on throughfall dynamics under pine and birch trees at the rainfall event level. *Atmosphere*, 8(12), 240. <https://doi.org/10.3390/atmos8120240>

How to cite this article: Lüpke M, Leuchner M, Levía D, Nanko K, Iida S, Menzel A. Characterization of differential throughfall drop size distributions beneath European beech and Norway spruce. *Hydrological Processes*. 2019;1–16. <https://doi.org/10.1002/hyp.13565>

APPENDIX

TABLE A1 List of measured events and parameters for beech

No.	Pos.	D10 mm	D50 mm	D90 mm	RR _{mean} mm hr ⁻¹	RR _{max} mm hr ⁻¹	RA l m ⁻²	N	Δt min	Lvl
1	O	0.75	1.12	1.52	0.16	0.63	0.10	1,084	36	L
	F	0.46	0.59	0.67	0.00	0.01	0.00	28		
2	O	0.70	1.12	1.64	1.65	28.61	7.83	46,646	284	H
	F	0.73	2.46	3.60	1.39	21.39	6.59	46,746		
3	O	0.61	0.83	1.00	0.43	0.94	0.11	2,284	16	L
	F	0.61	1.51	2.08	0.05	0.16	0.01	140		
4	O	0.46	0.69	0.92	0.70	7.56	0.66	7,960	56	H
	F	1.09	2.38	3.70	0.36	1.69	0.34	3,095		
5	O	0.48	0.65	0.84	0.03	0.12	0.01	259	20	L
	F	0.59	0.74	0.80	0.00	0.00	0.00	3		
6	O	0.63	0.96	1.50	0.64	5.37	1.88	21,566	176	H
	F	0.68	2.04	2.90	0.26	1.24	0.76	7,171		
7	O	0.66	1.01	1.47	0.29	1.56	0.65	8,791	136	M
	F	0.57	1.60	2.03	0.08	1.04	0.18	1,867		
8	O	0.84	1.43	2.23	3.79	15.18	7.33	38,450	116	H
	F	0.69	2.98	5.12	2.91	8.81	5.63	44,692		
9	O	0.50	0.80	1.05	0.12	0.20	0.03	552	18	L
	F	0.55	0.82	0.95	0.00	0.00	0.00	16		
10	O	0.80	1.29	1.95	1.83	5.00	6.09	41,331	200	H
	F	0.74	2.88	4.76	1.46	3.91	4.88	36,252		
11	O	0.56	0.86	1.19	0.14	0.60	0.53	9,852	232	L
	F	0.67	1.09	1.29	0.02	0.25	0.07	757		
12	O	0.84	1.33	2.00	1.77	9.47	13.24	104,099	448	H
	F	0.74	2.98	4.89	1.37	7.02	10.22	80,537		
13	O	0.57	0.84	1.12	0.60	2.85	0.48	7,438	48	M
	F	1.33	2.38	2.74	0.13	0.46	0.10	587		
14	O	0.60	0.92	1.30	0.13	0.64	0.38	5,977	180	L
	F	0.59	0.92	1.07	0.01	0.25	0.03	319		
15	O	0.60	0.94	1.37	0.37	1.15	0.99	14,293	160	M
	F	0.82	2.50	3.25	0.28	2.85	0.73	3,831		
16	O	0.48	0.82	1.25	1.40	13.12	55.28	1,510,222	2368	H
	F	0.73	2.94	4.53	0.95	10.80	37.58	312,049		
17	O	0.54	0.83	1.18	0.24	0.57	0.08	1,394	20	L
	F	0.53	0.95	1.17	0.01	0.04	0.00	74		
18	O	0.72	1.07	1.64	0.18	0.52	0.14	1,932	48	L
	F	0.54	0.92	1.03	0.01	0.04	0.01	86		
19	O	0.83	1.33	1.88	0.56	6.30	1.58	8,667	168	H
	F	0.84	2.10	3.06	0.28	2.25	0.77	6,262		

Abbreviations: No., event number; Pos, disdrometer position (R: rainfall/tower, TF: throughfall/floor); Lvl, Intensity levels at different maximum rain rate (RR_{max}) are defined by light (L): RR_{max} < 1 mm hr⁻¹, medium (M): RR_{max} 1–5 mm hr⁻¹, strong (S): RR_{max} > 5 mm hr⁻¹; Δt, duration; RA, rain amount (l m⁻²); N, number of drops; RR_{mean}, mean rain rate (mm hr⁻¹); RR_{max}, maximum rain rate (mm hr⁻¹); D10, 10th percentile volume diameter (mm); D50, median volume diameter (mm); D90, 90% volume diameter (mm).

TABLE A2 List of measured events and parameters for spruce

No.	Pos.	D10 mm	D50 mm	D90 mm	RR _{mean} mm hr ⁻¹	RR _{max} mm hr ⁻¹	RA l m ⁻²	N	Δt min	Lvl
20	O	0.42	0.67	0.93	0.18	2.02	0.23	6,757	80	M
	F	0.54	0.95	1.22	0.03	0.16	0.04	1,053		
21	O	0.51	0.79	1.14	0.29	2.51	0.34	4,665	72	M
	F	0.45	0.64	0.81	0.03	0.24	0.04	771		
22	O	0.67	1.17	1.93	1.50	3.68	0.80	9,108	32	M
	F	0.43	0.75	1.41	0.17	0.37	0.09	3,204		
23	O	0.76	1.15	1.68	3.17	9.71	2.11	13,742	40	H
	F	0.57	1.67	2.69	1.05	2.88	0.70	17,884		
24	O	0.46	0.71	0.94	0.12	0.29	0.02	668	12	L
	F	0.46	0.69	1.05	0.01	0.02	0.00	82		
25	O	0.55	0.82	1.15	0.24	1.27	0.47	8,025	120	M
	F	0.51	0.74	0.99	0.03	0.23	0.06	2,120		
26	O	0.42	0.65	0.88	0.04	0.19	0.05	1,817	72	L
	F	0.44	0.71	0.84	0.00	0.02	0.00	160		
27	O	0.46	0.67	0.81	0.08	0.21	0.04	1,320	28	L
	F	0.51	0.63	0.76	0.02	0.07	0.01	294		
28	O	0.52	0.84	1.15	0.19	1.28	1.03	19,736	320	M
	F	0.45	0.70	1.00	0.03	0.23	0.13	4,535		
29	O	0.56	0.88	1.28	0.64	6.81	3.75	42,251	352	H
	F	0.59	1.43	2.20	0.24	1.88	1.38	30,733		
30	O	0.48	0.76	1.07	0.09	0.70	0.25	5,517	160	L
	F	0.61	0.89	1.18	0.02	0.17	0.06	1,699		
31	O	0.70	1.08	1.50	0.85	3.14	0.91	10,943	64	M
	F	0.39	0.64	1.08	0.05	0.16	0.05	2,373		
32	O	0.43	0.71	1.04	0.44	4.39	6.41	201,947	876	M
	F	0.45	1.30	2.19	0.19	1.09	2.82	78,447		

Abbreviations: No., event number; Pos, disdrometer position (O: rainfall/tower, O: throughfall/floor); Lvl, Intensity levels at different maximum rain rate (RR_{max}) are defined by light (L): RR_{max} < 1 mm hr⁻¹, medium (M): RR_{max} 1–5 mm hr⁻¹, strong (S): RR_{max} > 5 mm hr⁻¹; Δt, duration; RA, rain amount (l m⁻²); N, number of drops; RR_{mean}, mean rain rate (mm hr⁻¹); RR_{max}, maximum rain rate (mm hr⁻¹); D10, 10th percentile volume diameter (mm); D50, median volume diameter (mm); D90, 90% volume diameter (mm).

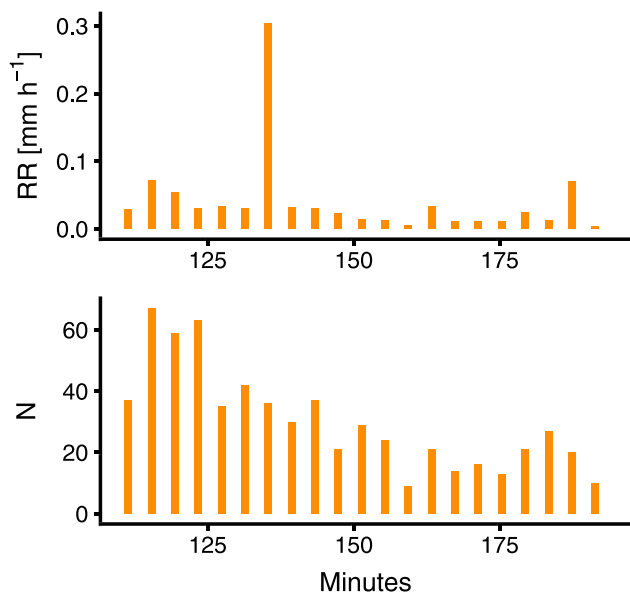


FIGURE A1 Intraevent variation of drop size distribution parameters during event 2 for beech of subevent 2 at open and floor measurement position (see also Table 2). (Top panel) rain rate (RR: mm hr⁻¹) for 4-min intervals; (Bottom panel) current number of drops per 4-min interval